catalysts

MDPI

Article

Photoelectrocatalytic Oxidation of Sulfamethazine on TiO_2 Electrodes

Nikolaos Philippidis [1], Eleni Pavlidou [2], Sotiris Sotiropoulos [1], Petros Kokkinos [3,4], Dionissios Mantzavinos [3] and Ioannis Poulios [1,*]

[1] Laboratory of Physical Chemistry, Department of Chemistry, Aristotle University of Thessaloniki, 54124 Thessaloniki, Greece; nikfilip@hotmail.com (N.P.); eczss@chem.auth.gr (S.S.)
[2] Department of Physics, Aristotle University of Thessaloniki, 54124 Thessaloniki, Greece; elpavlid@auth.gr
[3] Department of Chemical Engineering, University of Patras, University Campus, Caratheodory 1, 26504 Patras, Greece; pkokkin@upatras.gr (P.K.); mantzavinos@chemeng.upatras.gr (D.M.)
[4] School of Sciences and Engineering, University of Nicosia, 2417 Nicosia, Cyprus
* Correspondence: poulios@chem.auth.gr; Tel.: +30-2310997785

Abstract: The photoelectrocatalytic degradation and mineralization of sulfamethazine (SMT), a sulfonamide drug, were explored in aqueous solution. Working electrodes with TiO_2 coatings on Ti substrates (TiO_2/Ti) were used, which were produced by the dip coating method. TiO_2 film electrodes were analyzed by scanning electron microscopy (SEM) and X-ray diffraction (XRD) following annealing at 500 °C for 1.5 h. To photoelectrochemically characterize them, photocurrents vs. applied potential curves were used. The photoelectrocatalytic efficiency (PEC) of the TiO_2/Ti electrodes regarding the oxidation of SMT has been assessed with reference to degradation and mineralization under different experimental conditions. The selected drug molecule was effectively degraded following the Langmuir–Hinshelwood (L-H) kinetic model. The degradation efficiency was shown to increase with increasing applied potential bias up to +1.5 V vs. Ag/AgCl. It was found to be more favorable in acidic environments compared to alkaline ones. A decrease in the destruction rate constant was recorded when the pH was increased from 3 to 5.6 (natural pH) and 9. The decomposition rate was shown to first increase and subsequently reach a saturation value at high concentrations of SMT, indicating that the degradation also depends on other parameters (e.g., the rate of the charge or the mass transfer on the electrode double layer). The results of the photoelectrocatalytic experiments were compared to those of electrochemical (EC) and photocatalytic (PC) degradation of SMT. A significant enhancement was recorded in the case of the PEC degradation, leading at +1.5 V to an increase of the apparent rate constants of degradation, k, and mineralization, k_{TOC}, of 153 and 298%, respectively, compared to the simple photocatalytic process.

Keywords: photoelectrocatalysis; TiO_2; sulfamethazine; drugs

check for updates

Citation: Philippidis, N.; Pavlidou, E.; Sotiropoulos, S.; Kokkinos, P.; Mantzavinos, D.; Poulios, I. Photoelectrocatalytic Oxidation of Sulfamethazine on TiO_2 Electrodes. *Catalysts* **2023**, *13*, 1189. https://doi.org/10.3390/catal13081189

Academic Editor: Vincenzo Baglio

Received: 30 June 2023
Revised: 31 July 2023
Accepted: 3 August 2023
Published: 7 August 2023

Copyright: © 2023 by the authors. Licensee MDPI, Basel, Switzerland. This article is an open access article distributed under the terms and conditions of the Creative Commons Attribution (CC BY) license (https://creativecommons.org/licenses/by/4.0/).

1. Introduction

Research efforts in the water purification field are continuously growing since water quality control and regulations on different hazardous pollutants have become stricter [1].

Semiconductor photocatalysts offer a simple and cheap process for the abatement of organic compounds under artificial or solar light, and thus an increase in their use has been recorded during the last twenty years [2–4]. Because of its interesting characteristics (i.e., chemical stability against both corrosion and photocorrosion and good photocatalytic activity, particularly in its anatase form), titanium dioxide (TiO_2) has been extensively studied and applied, commonly in the form of a slurry of fine particles in a photochemical reactor. The slurry offers a high photoinduced reaction surface and a low recombination rate of the photogenerated e^-/h^+ pairs, resulting in high purification efficiency. However, TiO_2 particles cannot be easily separated from the treated wastewater, requiring high operation costs and a complex treatment system. To prevent the need for a separation step,

TiO_2 particles may be immobilized onto supporting materials, despite the fact that due to the decrease in catalyst surface area and the diffusion limitations of the organic substance to the catalyst, a decrease in oxidation efficiency is recorded. Different approaches have been investigated to face this problem (e.g., TiO_2 was supported on an electronic conductor and biased positive with the application of an external voltage in a photoelectrochemical cell). In this way, the rate of the photogenerated electron–hole recombination is restricted, and the rate of the surface reactions increases (photoelectrocatalytic oxidation) [5–8].

SMT is a main sulfonamide antibiotic with a functional group of $–SO_2NH_2–$. It is broadly used for the control of infectious diseases and for the growth of animals [9,10]. Due to its wide spectrum of antibacterial efficacy and low cost, it is frequently prescribed to humans, aquaculture, and livestock [11,12]. SMT is resistant to biodegradation due to the sulfonamide group, which can inhibit the growth of many Gram-negative and Gram-positive bacteria [13]. Heterocyclic sulfonamides (SAs) are an important group of pharmaceuticals, being the most frequently detected antibiotics in surface waters and wastewaters, followed by fluoroquinolones, tetracyclines, and macrolides [11,14–16]. They have been in constant use since the 1930s, posing a significant contamination risk. SMT has been detected in various aquatic matrices, such as groundwater, seawater, and river water, as well as in treated water effluent and reclaimed water [17,18]. It is also persistent and able to accumulate in organisms and soils, and it has been detected in sediments, animal manure, and manure waste lagoons [16,17,19]. SAs have been receiving increasing attention because they can adversely affect both the health of humans and ecosystems [9,17,20,21]. Because SMT interrupts the human endocrine system, may be harmful to marine species, and affects animal reproduction, its presence in aquatic environments is of concern [12]. In addition, its environmental prevalence enhances the spread of resistance in microorganisms, ultimately influencing the efficiency of treatment [22]. Environmental SMT concentrations generally range from nanograms per liter to micrograms per liter [10,12,18,20,21]. SMT concentrations in the range of 15–328 ng/L and 2.05–623.27 ng/L have been detected in tropical waters in Vietnam and river water in China, respectively [10,23]. Other studies reported that SMT was found in water from wells and rivers in concentrations ranging from 0.22 to 2.48 μg/L, respectively [24].

Conventional processes (e.g., coagulation, flocculation, and sedimentation) have been proven inefficient towards the abatement of antibiotics, while physical approaches, such as adsorption, ultrafiltration, and reverse osmosis, are known to be non-destructive, thus transferring pollutants from one phase to another, finally resulting in secondary pollution [10,11,24]. Numerous alternative treatment technologies have been evaluated for the degradation of these emerging organic pollutants [12,23–26]. Advanced oxidation processes (AOPs) (photo-Fenton, electro-Fenton, sonolysis, etc.) have been proven very effective and are characterized by high rates of degradation in a short time [10,13,26,27]. However, some of them are characterized by high processing costs due to the required energy and/or the production of extra waste (e.g., iron-containing sludge) [9,10]. Thus, the development of a cost-effective, environmentally friendly treatment process for the successful abatement of SMT and other antibiotics and organic pollutants from aquatic bodies is of high importance. Due to its very interesting characteristics (high degradation efficiency, potential for solar energy use, mild conditions of reactions, absence of harmful by-products, and effective catalyst recovery), photoelectrocatalysis (PEC) has been proven to be a promising emerging AOP [17,18,20,28].

However, studies of photoelectrocatalysis (PEC) abatement of SMT are still few. The first report on photo-electrocatalytic degradation of SMT by semiconductor MOFs as catalysts was by Jia et al. (2020). The rate of reaction of ZIF-8/NF-TiO_2 increased by 21.7 times compared with unmodified anatase TiO_2, while the synergistic factor in the photo-electrocatalytic process could reach 3.5 [16]. Recently, three studies on PEC SMT degradation have been reported [18,28,29]. Candia-Onfray et al. (2023) produced various MOF-derived photoanodes ($Ru_3(BTC)_2$, UiO-66(Zr) NH_2, and Au@ZIF-8, on Ti/TiO_2NT) and applied them for the photo(electro) chemical abatement of CECs, including SMT, in a

spiked secondary effluent sample from a municipal wastewater treatment plant [29]. In another study, Wu et al. (2023) produced a series of Bi-Ti/powdered activated carbon (PAC) composites by the sol-hydrothermal method and studied the adsorption and photocatalytic degradation of SMT [28]. An additional recent photoelectrocatalytic study was described by Hu et al. (2023), who produced a self-driven dual-photoelectrode PEC system (TiO_2 NNs-Co_3O_4) made of a TiO_2 nanoneedle array (TiO_2 NNs) photoanode and Co_3O_4 photocathode, which was used for the degradation of SMT [18].

Our present study provides results describing the production of TiO_2 electrodes on Ti substrates, their characterization, and the study of their photoelectrocatalytic activity towards the degradation of SMT, whose structure is shown in Figure 1. The photoelectrocatalytic oxidative degradation of SMT was studied under artificial illumination in a novel photoelectrocatalytic reactor, and different parameters such as pH, concentration of the target drug molecule, and applied potential were investigated. We also aimed to compare the results of the photoelectrocatalytic experiments to those of electrochemical (EC) and photocatalytic (PC) degradation of SMT.

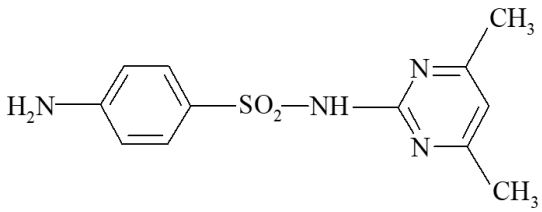


Figure 1. Chemical structure of Sulfamethazine (CAS 57-68-1).

2. Results

2.1. Photoelectrochemical Behavior of the TiO_2/Ti Electrode in Supporting Electrolyte

Figure 2 shows the XRD pattern of the TiO_2/Ti electrode (annealed for 1.5 at 500 °C). A high intensity peak at 2θ = 25.28° and a low intensity peak at 2θ = 28.06°correspond to anatase TiO_2 and the rutile phase, respectively. In accordance with the starting Degussa P-25 material specifications, the anatase form of TiO_2 was predominant in the TiO_2/Ti film. Figure 3 shows the surface morphology of the particulate TiO_2/Ti working electrode. A network of spherical aggregates of a few μm was found. Following annealing, a few tens of nm P-25 particles (ca. 30 nm) have merged into these aggregates.

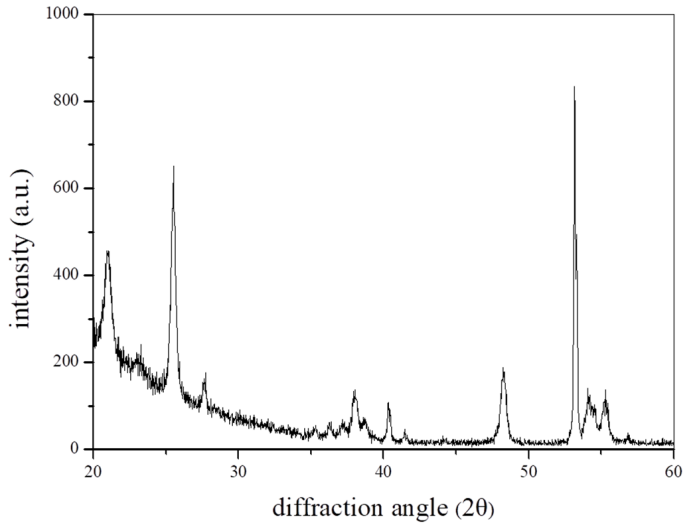


Figure 2. XRD diffractogram of the TiO_2/Ti specimen after annealing at 500 °C for 1.5 h.

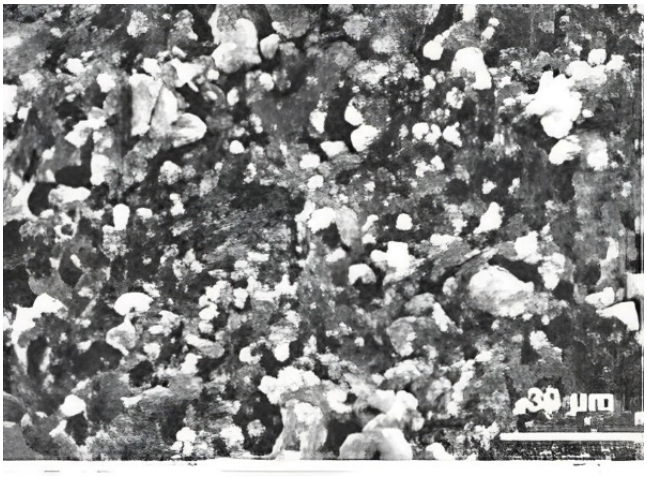


Figure 3. Scanning electron microscopy (SEM) micrograph of the particulate TiO_2/Ti specimen after annealing at 500 °C for 1.5 h.

The current–potential curves of the particulate TiO_2/Ti electrode in 0.1 M Na_2SO_4, under dark conditions, and under UV-A illumination (within the potential range of −0.5 and +2 V vs. Ag/AgCl) are shown in Figure 4.

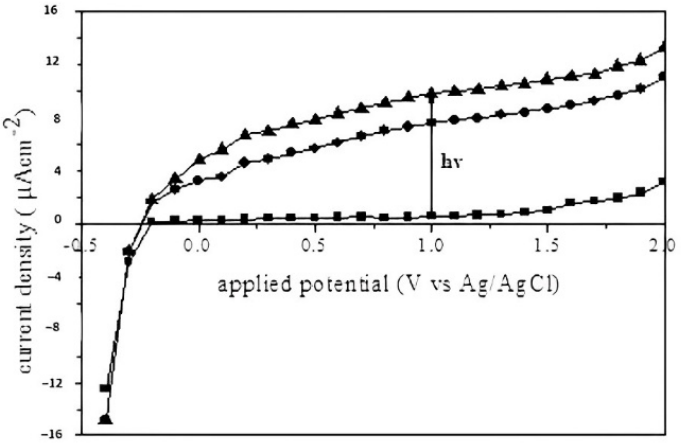


Figure 4. I-V voltammograms for the TiO_2/Ti electrode at pH = 5.6, in 0.1 M Na_2SO_4, in the dark (■), under illumination in 0.1 M Na_2SO_4 (●) and under illumination in 0.1 M Na_2SO_4 + 20 mg L^{-1} SMT (▲).

The TiO_2/Ti electrode exhibits nearly perfect blocking characteristics in the potential range of −0.2 to +1.6 V vs. Ag/AgCl, typically for an n-type semiconductor (Figure 4). Also, due to water decomposition and oxygen evolution, an increase in dark current density has been recorded for potentials higher than +1.6 V.

Contrarily, a remarkable increase in the anodic current density was shown above −0.2 V vs. Ag/AgCl upon illumination. In accordance with the bibliography [30–33], the illumination of a semiconductor–electrolyte interface with light energy higher than that of its band gap energy results in the production of electron–hole pairs (e^-/h^+) in the space charge layer of the semiconductor. The contemporaneous application of a bias potential positive to the flat-band potential generates a bending of the conduction and valence bands, resulting in a more efficacious separation of the photogenerated carriers within the space charge layer. It also augments the photocurrent (I_{ph}) that begins to flow and likely promotes the oxidative degradation process. The potential gradient effectively forces the electrons to arrive at the counter electrode and leave the photogenerated holes to react with H_2O/OH^- to produce $OH^\bullet$ radicals or to directly react with the organics presented in the solution, as shown by the global reactions described by Equations (1)–(5).

Anode (working electrode):

$$TiO_2 + h\nu\ (<400\ nm) \rightarrow TiO_2 - e^-{}_{cb} + TiO_2 - h^+{}_{vb} \quad (1)$$

$$TiO_2 - h^+{}_{vb} + H_2O_s \rightarrow TiO_2 - OH_s^\bullet + H^+ \quad (2)$$

$$TiO_2 - h^+{}_{vb} + OH^-{}_s \rightarrow TiO_2 - OH_s^\bullet \quad (3)$$

$$TiO_2 - e^-{}_{cb} + TiO_2 - h^+{}_{vb} \rightarrow \text{recombination} \quad (4)$$

Cathode (counter electrode):

$$2H_2O + 2e^- \rightarrow H_2 + 2OH^- \quad (5)$$

cb and vb denote the conduction band and valence band of the photocatalyst, while h^+ and e^- correspond to the photogenerated holes and electrons, respectively.

2.2. Bulk Photoelectrocatalytic Oxidation of Sulfamethazine at the TiO_2/Ti Electrodes

The change in the absorption spectrum of 20 mg L^{-1} (7.8×10^{-5} M) SMT during its photoelectrocatalytic abatement at an anodic bias of +1.5 V vs. Ag/AgCl in a 0.1 M Na_2SO_4 solution is shown in Figure 5. The increase in illumination time results in a decrease in the intensity of the absorption maximum at 264 nm, which disappears almost completely within ~3 h, indicating the complete decomposition of the SMT molecule.

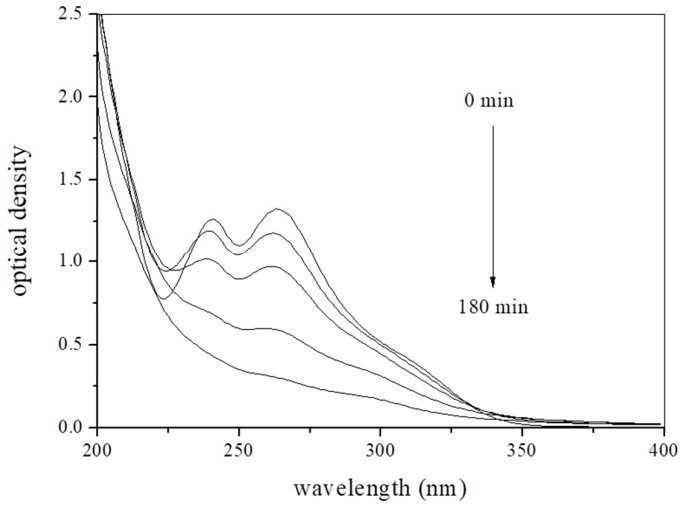


Figure 5. UV-Vis absorption spectra of SMT (20 mg L^{-1} SMT, 0.1 M Na_2SO_4, pH 5.6) during the photoelectrocatalytic abatement at different reaction times on the TiO_2/Ti electrode at +1.5 V vs. Ag/AgCl applied potential.

Figure 6, on the other hand, shows the performance of the TiO_2/Ti electrode in regard to the reduction of the drug concentration in relation to the illumination time under various experimental conditions. The relative decrease is the ratio of SMT concentration at time t to its starting concentration in the solution at t = 0. Three distinct groups of conditions were investigated: (a) the photocatalytic degradation efficiency without any applied potential; (b) the electrochemical degradation by biasing the electrode with +1.5 V in the dark; and (c) the photoelectrocatalytic degradation, i.e., applying both a +1.5 V potential and UV-A light. As shown in Figure 6 and in Table 1, where the apparent reaction rate constants of degradation (k) under the different experimental conditions are provided, direct electrochemical oxidation contributed less than 5% to the SMT abatement after 3 h. The pure photocatalytic process, that is, without applying potential, corresponding to the open circuit conditions, resulted in a 72% decrease in SMT concentration after 3 h of

illumination. However, when applying an anodic potential of +1.5 V, the photodegradation efficiency was enhanced to 97%, indicating that the applied potential increases the SMT degradation rate remarkably.

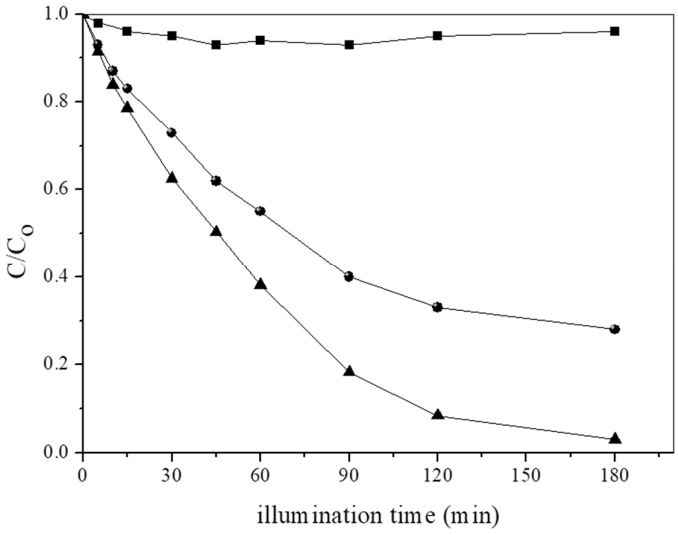


Figure 6. Degradation of SMT on a TiO_2/Ti electrode in relation to illumination time: (■) electrochemical oxidation at E = +1.5 V vs. Ag/AgCl; (●) photocatalytic oxidation under UV-A light without potential; and (▲) photoelectrocatalytic oxidation under UV-A light and V= +1.5 V vs. Ag/AgCl. In all cases, the SMT concentration was 20 mg L^{-1} in 0.1 M Na_2SO_4 at pH 5.6.

Table 1. Apparent rate constants of degradation, k, and mineralization, $k_{DOC,}$ of 20 mg L^{-1} SMT in a 0.1 M Na_2SO_4 solution under different experimental conditions.

Experimental Conditions	Apparent Rate Constant of Degradation k × 10^3 (min^{-1})	Apparent Rate Constant of Mineralization k_{DOC} × 10^3 (min^{-1})
Photoelectrocatalytic, pH = 5.6, +1.5 V vs. Ag/AgCl	15.65 ± 0.28	4.63 ± 0.06
Photoelectrocatalytic, pH = 3, +1.5 V vs. Ag/AgCl	20.84 ± 0.30	5.78 ± 0.09
Photoelectrocatalytic, pH = 9, +1.5 V vs. Ag/AgCl	11.7 ± 0.34	2.97 ± 0.31
Electrochemical, +1.5 V vs. Ag/AgCl	2.65 ± 0.34	-
Photocatalytic, pH = 5.6	10.2 ± 0.42	1.55 ± 0.22
TiO_2/Pt, Photoelectrocatalytic, pH = 5.6, +1.5 V vs. Ag/AgCl	28.32 ± 1.16	8.51 ± 0.74
Thermal-TiO_2/Ti, Photoelectrocatalytic, pH = 5.6, +1.5 V vs. Ag/AgCl	16.62 ± 1.83	0.95 ± 0.06
Photoelectrocatalytic, pH = 5.6, +0 V vs. Ag/AgCl	12.74 ± 1.36	1.85 ± 0.12
Photoelectrocatalytic, pH = 5.6, +1.0 V vs. Ag/AgCl	13.49 ± 1.6	2.32 ± 0.19

Similarly to other organic pollutants, SMT photodecomposition is a complex process with many intermediate products, which can be characterized by higher toxicity compared to the parent compounds, thus being of high importance in water treatment processes. Consequently, it is of crucial importance to achieve complete mineralization of the organic pollutants by applying the selected method. The general equation, which describes the complete SMT oxidation (mineralization), is shown in Equation (6) and is valid after a prolonged irradiation time:

$$C_{11}H_{14}O_2N_4S + 20\ O_2 \rightarrow \text{intermediates} \rightarrow 11CO_2 + 4NO_3^- + SO_4^{2-} + 6H^+ + 4H_2O \quad (6)$$

A detailed photoelectrocatalytic SMT oxidation mechanism has been described in previous studies [34–36]. A composite of g-C_3N_4 with TNTs (g-C_3N_4/TNTs) has been developed in the study of Ji et al. (2020), showing high photocatalytic efficiency for SMT degradation under simulated solar light, 100% removal within 5 h, decreased toxicity of degradation intermediates/products, a high mineralization rate, and good reusability [26].

Figure 7 shows the level of mineralization as the dissolved organic carbon (DOC) reduction vs. time of illumination for a solution containing 20 mg L^{-1} SMT, and Table 1 shows the apparent reaction rate constants of mineralization (k_{DOC}) under the same experimental conditions as Figure 6. The photoelectrocatalytic oxidation at +1.5 V results in a 63% reduction of the initial carbon content of SMT after 4 h of illumination. At the same time, the decomposition was almost complete, indicating the presence of difficult degradable intermediates (Figure 6). For simple photocatalytic oxidation, as in the degradation results, the photomineralization is less efficient in comparison to the one when an anodic potential is applied. Only 26% of the initial organic content contained in the SMT molecule is converted to CO_2 at the same time as the reaction. Under the given experimental conditions, electrochemical oxidation proves to be a very inefficient process of degradation and mineralization of the target molecule.

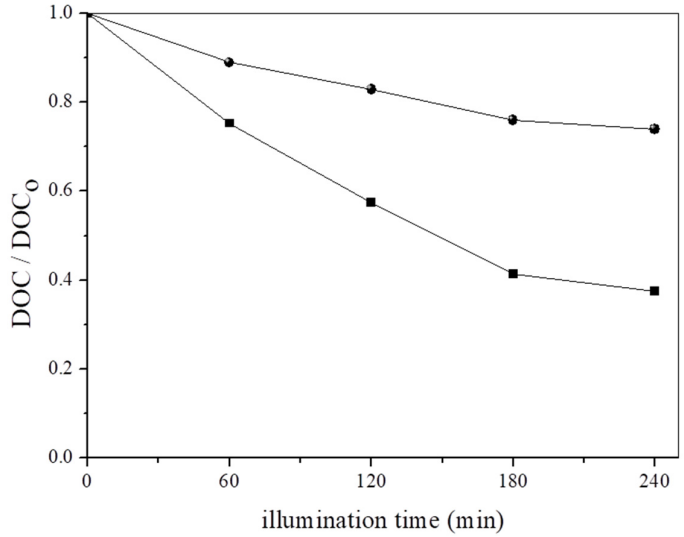


Figure 7. Mineralization of SMT on a TiO_2/Ti electrode in relation to illumination time: (●) photocatalytic oxidation under UV-A light without applied potential; (■) photoelectrocatalytic oxidation under UV-A light; and V = +1.5 V vs. Ag/AgCl. In all cases, the SMT concentration was 20 mg L^{-1} in 0.1 M Na_2SO_4 at pH 5.6.

Experimental data show that photoelectrocatalytic processes are more effective compared to pure electrochemical or photocatalytic ones for drug degradation. An anodic potential higher than that of the flat band potential of TiO_2 results in a significant increase in the efficiency of the photocatalytic activity of the Ti/TiO_2 electrode and consequently increases the reaction rate of SMT degradation. As mentioned before, the application of the positive potential to the TiO_2/Ti electrolyte interface gives a potential gradient within the semiconductor layer, which can drive the photogenerated holes and electrons efficiently apart. Therefore, the charge recombination of the photogenerated carriers decreases, and thus a higher number of positively charged holes is available for the photooxidation of H_2O or the SMT molecule and the intermediate products adsorbed onto the surface of TiO_2.

A few recent studies on PEC SMT degradation have been published. In the study of Candia-Onfray et al. (2023), higher degradation percentages were recorded for Ti/TiO_2NT-

$Ru_3(BTC)_2$ after PEC treatment of 180 min, resulting in the removal of a total concentration of CECs higher than 90%. According to the authors, this finding could be attributed to the higher production of •OH generated by the UV irradiation and the stabilization of the photogenerated charge by the applied current [29]. The Bi-Ti/PAC photocatalyst with a Bi/Ti molar ratio of 10% and calcination temperature of 400 °C was the most efficient in the study of Wu et al. (2023), was stable, and could be recycled for many SMT degradation rounds. SMT degradation rate reached 81.18% (time: 300 min, catalyst dosage: 1.0 g/L, initial SMT concentration: 20 mg/L, pH: 6.0, visible light irradiation at wavelength: 400–780 nm, pseudo first-order rate constant: 0.00531 min^{-1}, regression coefficient of 0.99682) [28]. Finally, Hu and colleagues (2023) showed that under light-emitting diode (LED) illumination, the bias-free TiO_2 NNs-Co_3O_4 PEC system showed exceptional PEC performance, with an internal bias as high as 0.19 V, resulting in almost complete degradation (99.62%) of SMT, with a pseudo-first-order rate constant of 0.042 min^{-1}, showing also excellent reusability performance (99.40% of the fifth cycles) [18].

The rate of the photoelectrocatalytic degradation of SMT at the TiO_2/Ti electrode is affected by different parameters, such as the initial SMT concentration pH, applied potential, light intensity, etc., and some of these factors are discussed below.

Figure 8A shows the effect of the initial SMT concentration on the initial reaction rate (r_o) of photodegradation and mineralization. The r_o values were independently obtained by a linear fit of the C-t data in the range of 10–50 mg L^{-1} initial SMT concentration. To minimize variations because of the competitive effects of intermediates, pH changes, etc., the calculations of the initial reaction rates were based only on experimental data collected during the first 45 min of illumination. The curve is reminiscent of a Langmuir type isotherm, at which the decomposition rate first increases and subsequently reaches a saturation value at high concentrations of SMT, indicating that the degradation also depends on other parameters, such as, for example, the rate of the charge or the mass transfer on the electrode double layer.

The photocatalytic degradation rate of organic compounds is usually described by a pseudo-first-order kinetic expression, which is rationalized in terms of the Langmuir-Hinshelwood (L-H) model, modified to accommodate reactions occurring at the solid-liquid interface [37,38].

$$r_o = -\frac{dC}{dt} = \frac{k_r K C}{1 + KC} \quad (7)$$

where r_o is the initial rate of disappearance of the organic substrate, C is the initial bulk-solute concentration, K corresponds to the equilibrium constant of adsorption of the organic substrate onto TiO_2, and k_r reflects the limiting rate constant of reaction at maximum coverage under the given experimental conditions. This equation can be used when data exhibit sufficient linearity when plotted as follows:

$$\frac{C}{r_o} = \frac{1}{k_r K} + \frac{C}{k_r} \quad (8)$$

Figure 8B shows the dependence of C/r_o values on the respective initial SMT concentrations. The k_r and K values calculated according to Equation (8) from the slope of the straight line (R^2 = 0.99) and from the intercept with the C/r_o axis were 0.47 mg L^{-1} min^{-1} and 0.05 mg L^{-1}, respectively.

Figure 9 presents the effect of the applied potential on the degradation (A), and mineralization (B) of 20 mg L^{-1} SMT, while in Table 1, the k and k_{TOC} values under the different potential values are given. As can be seen, an increase in cell voltage leads to an increase in the kinetic constants of degradation and mineralization. By applying +1.5 V, the k and k_{TOC} values increased by 123% and 250% compared to 0 V cell voltage, respectively, while a 153 % increase in k and a 298% increase in k_{TOC} were attained in comparison to the simple photocatalytic process. This finding supports the fact that the applied potential is a key factor for photoelectrocatalytic oxidation.

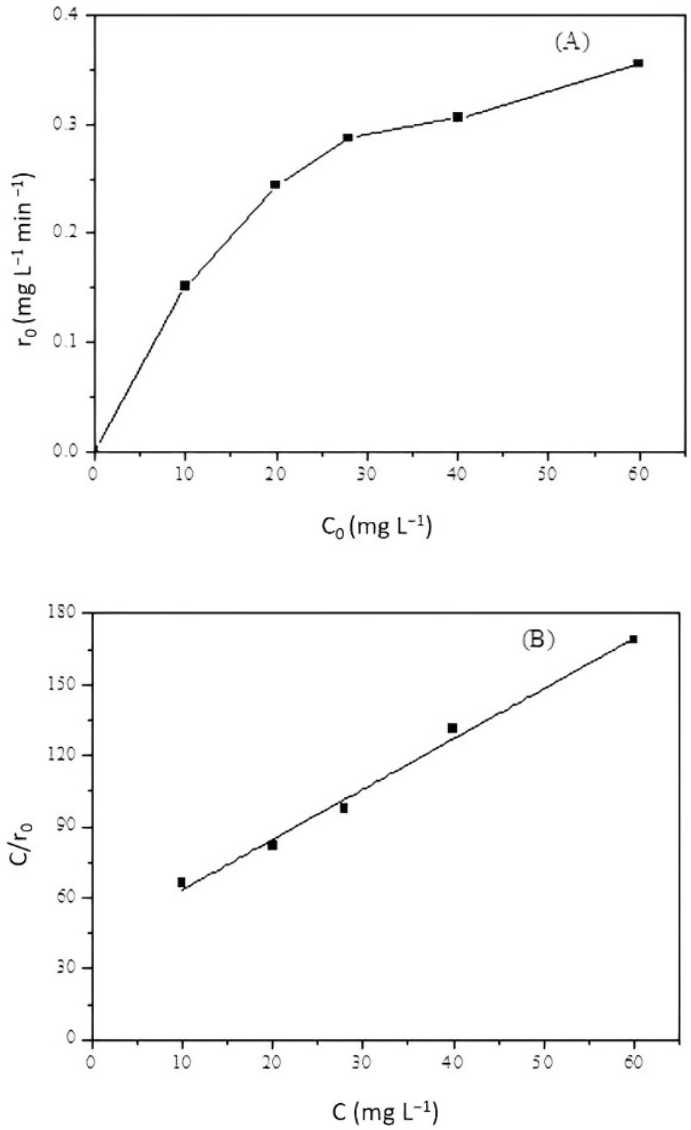


Figure 8. (**A**) Plot of ro vs. C at different initial SMT concentrations from 10 to 60 mg L^{-1} at +1.5 V vs. Ag/AgCl. (**B**) linear transform of C/r_o vs. C according to Equation (8).

As a result, as the potential increases up to +1.5 V, the rate of SMT oxidation increases, while additionally increasing the potential beyond this value does not enhance the degradation rate. The conditions applied in synthesizing the photoelectrode dictate the potential at which the maximum rate of degradation is achieved, but according to the literature, it seems to be no higher than 2 V. If the potential exceeds this value, this triggers direct electrooxidation of H_2O or SMT.

2.3. The Effect of pH on the Degradation of Sulfamethazine

The solution pH influences the speciation of both the surface functional groups of the TiO_2/Ti electrode and the chemical forms of organic compounds in the solution [39,40]. The solution pH also influences the flat band potential, increasing it by 59 mV per pH unit in the cathodic direction [32], therefore decreasing the oxidative power of the photogenerated holes. All of these pH-dependent parameters may influence the photoelectrocatalytic oxidation of an organic molecule at the TiO_2 electrode.

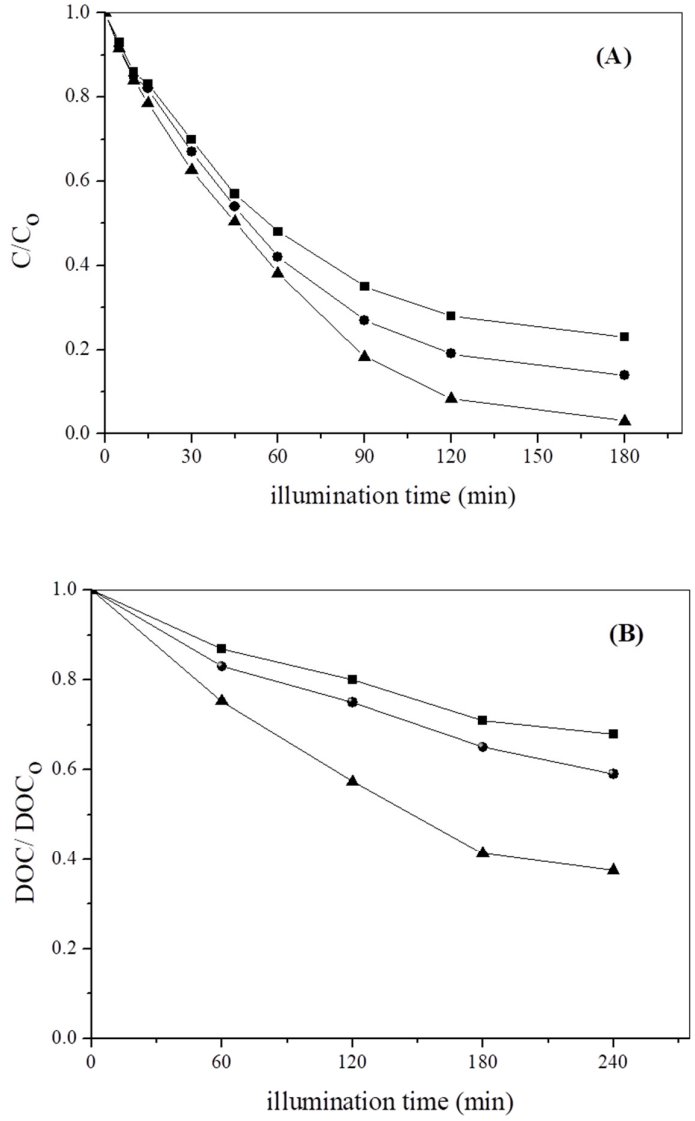


Figure 9. Degradation (**A**) and mineralization (**B**) of SMT on a TiO_2/Ti electrode as a function of illumination time at different applied potentials vs. Ag/AgCl: (■) 0 V, (●) +1 V and (▲) +1.5 V. In all cases, the SMT concentration was 20 mg L^{-1} (10.34 mg L^{-1} DOC) in 0.1 M Na_2SO_4.

The effect of the initial solution pH on the degradation (A) and mineralization (B) of 20 mg L^{-1} SMT is shown in Figure 10, while the k and k_{DOC} values under the different pH values are provided in Table 1. An applied potential across the photoanode/electrolyte interface of +1.5 V and a supporting electrolyte concentration of 0.1 M were used for all experiments. As can be seen in both Figure 10 and Table 1, as it concerns SMT degradation, a decrease in the destruction rate constant was recorded when the pH was increased from 3 to 5.6 (natural pH) and 9. This finding is in line with Yang's results on pentachlorophenol degradation [41], as well as with Kim and Anderson's findings [42], where the maximum photoelectrocatalytic degradation of HCOOH was recorded at pH = 3.4.

A novel clay (bentonite)-supported Ag^0 nanoparticles (NPs)-doped TiO_2 nanocomposite (Clay/TiO_2/Ag^0 (NPs) thin film) was applied for the photocatalytic breakdown of SMT from aqueous solution under visible light and UV-A radiation. It has been shown that pH 6 was the maximum pH value for an efficient SMT breakdown, while the reduction in antibiotic concentration (0.5–20.0 mg/L) highly supported the degradation efficiency, with the process following pseudo-first-order kinetics [12]. Graphene modified anatase/titanate nanosheets (G/A/TNS) were applied for solar-light-driven photocatalytic breakdown of

SMT, resulting in a degradation of 96.1% in 4 h at pH 6, with a pseudo-first-order model describing the reaction kinetics and a rate constant (k1) for SMT degradation by G/A/TNS-0.5 of 0.493 h^{-1} [43]. The kinetics of photo-decomposition of SMT in the absence and presence of TiO_2 at pH 3, 5.5, and 10 were also assessed by Tzeng et al. (2016). Apparent rate constants were well described by the pseudo-first-order kinetic model and ranged from 0.24 to 1.61 h^{-1}. It has been shown that photolytic reactions dominate SMT decomposition at pH 10. However, the overall photo-decomposition was increased at pH 5.5 because the SMT adsorption on TiO_2 surfaces was significantly enhanced, supporting the photo-catalytic degradation of SMT by OH radicals [9]. Ayala-Durán et al. (2020) evaluated iron mining residue as a potential catalyst for heterogeneous Fenton/photo-Fenton degradation of sulfonamide antibiotics. Authors showed that degradation was significantly dependent on the initial pH value, with the highest efficiency recorded at pH 2.5, resulting in a concentration below the detection limit of sulfathiazole within 30 min (under black light irradiation, using 0.3 g L^{-1} residue, and H_2O_2 consumption of 0.2 mmol L^{-1}). Catalytic activity was maintained high during up to five cycles [44].

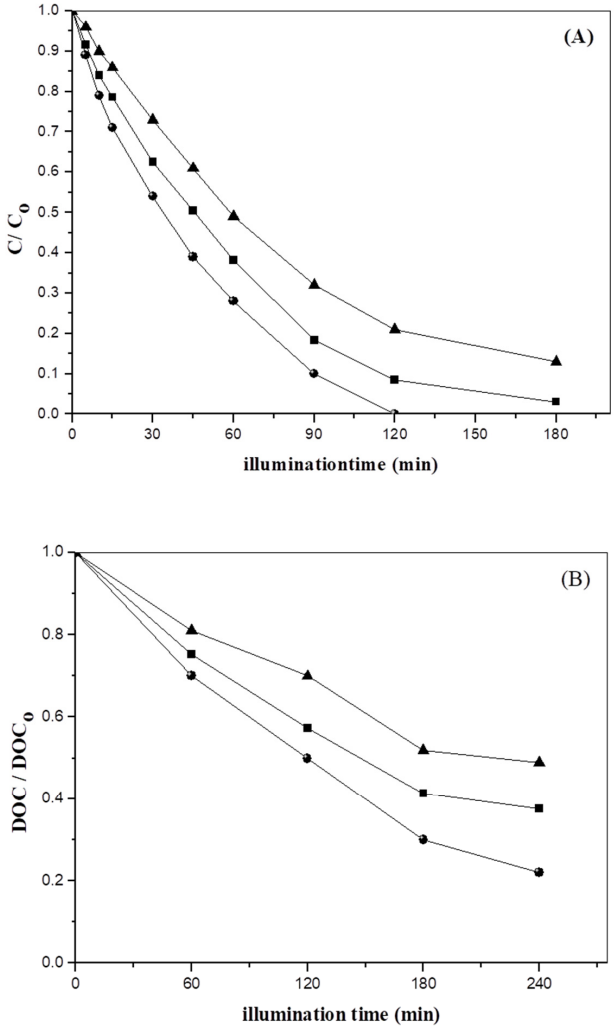


Figure 10. Degradation (**A**) and mineralization (**B**) of SMT on a TiO_2/Ti electrode as a function of the time of illumination at various initial pH values: (●) pH = 3, (■) pH = 5.6, and (▲) pH = 9. In all cases, the SMT concentration was 20 mg L^{-1} in 0.1 M Na_2SO_4.

2.4. The Effect of the Type of the Electrodes on the Degradation of Sulfamethazine

Additionally, experiments with P-25 TiO_2/Ti photoelectrodes, Pt-modified P-25 TiO_2/Ti, and thermally grown anatase photoanodes were also studied. The former were produced

by a photocatalytic method that involves the reduction of Pt ions onto a TiO_2 surface upon UV-A illumination [45]. The latter were thermally grown by sintering TiO_2 P-25 at 500 °C. As can be seen in Figure 11 and Table 1, the presence of Pt islands on the TiO_2 particles causes an increase in the photoelectrocatalytic efficiency due to the better charge transfer of the photogenerated carriers through the electrode layer. This leads to a complete reduction of the SMT molecules in the solution after just 90 min of illumination, while the associated reaction rate constant is significantly increased (see Table 1). On the contrary, the thermal electrode shows a weaker photoelectrocatalytic behavior, leading after 3 h only to a ~50% reduction of the SMT concentration and a 21% reduction of the dissolved organic carbon.

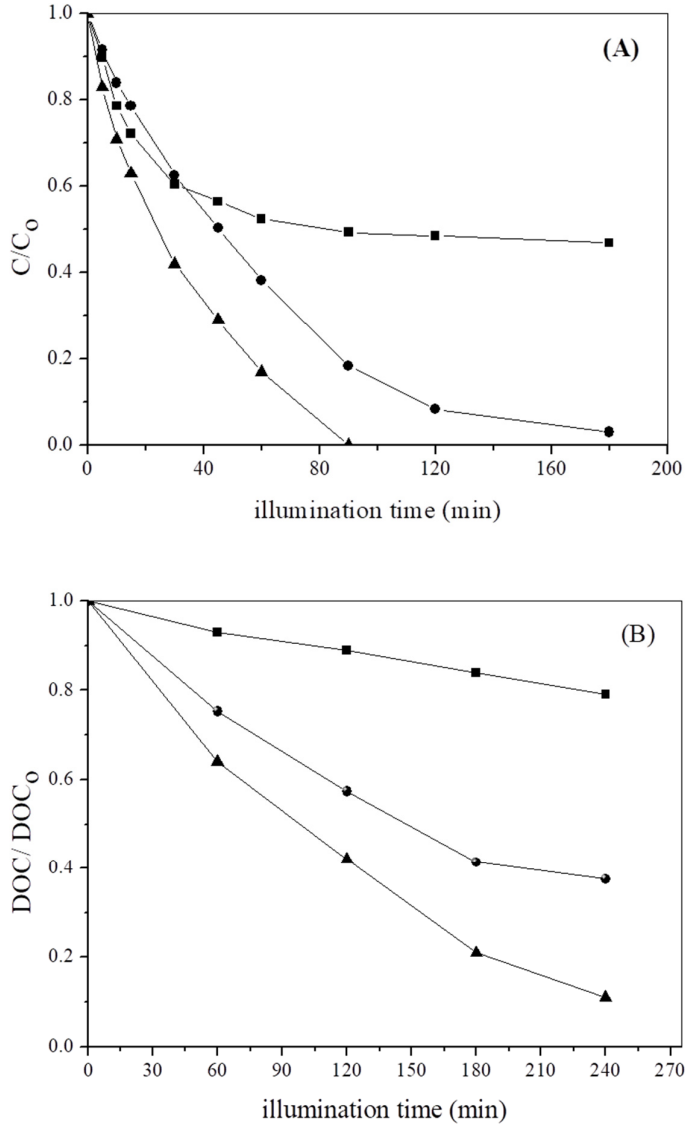


Figure 11. Photoelectrocatalytic degradation (**A**) and mineralization (**B**) of 20 mg L^{-1} SMT in 0.1 M Na_2SO_4 and pH 5.6 using different working electrodes. (▲) Pt-TiO_2/Ti, (●) TiO_2/Ti, and (■) thermal TiO_2/Ti. In all cases, the applied potential was +1.5 V vs. Ag/AgCl.

SMT photodegradation in the presence of TiO_2, P25, and ZnO under UV irradiation was examined by Aissani et al. (2018). Adsorption experiments in the dark showed no adsorption of SMT on the catalysts, while direct photolysis did not significantly degrade SMT. Moreover, the pH effect was negligible in the range 4–9, and the removal efficiency was found to be influenced by the amount of catalyst (optimal values were 0.5 and 0.25 g/L for TiO_2 P25 and ZnO, respectively). A negative effect on its degradation was caused by

an increase in the initial SMT concentration, while a second-order kinetic model described the experimental data in the presence of TiO_2 [10]. The photocatalytic degradation of SMT in TiO_2 suspension was studied both experimentally and theoretically under UV irradiation by Zhang (2014). SMT degradation was found to increase with prolonged reaction times [17]. Photolytic and photocatalytic degradation of SMT dissolved in Milli-Q water and in synthetic wastewater were described by Babić et al. (2015). Different processes were investigated, including direct photolysis, UV/H_2O_2, UV/TiO_2, and UV/TiO_2/H_2O_2 using UV-A and UV-C radiation. Pseudo-first-order kinetics were found to describe SMT degradation in all studied processes. UV-C/TiO_2/H_2O_2 was the most efficient process, resulting in a complete SMT abatement in only 10 min [15]. Large-area N-TiO_2/GR layer materials were found to exhibit enhanced photocatalytic activity for the degradation of different antibiotics, including SMT, with graphene being able to function as an effective "electron pump" for the photodegradation, which can enhance the separation of carriers [46]. A reactor composed of four consecutive stainless-steel plates immobilized by tungsten-doped TiO_2 ($WeTiO_2$) using polysiloxane has been constructed by Fouad et al. (2020) for the degradation of SMT. The residual SMT concentration was below the detection limit after 30 min of photocatalysis (initial concentration: 17.42 mg/L, flow rate: 300 mL/min, pH: 4.0) [23].

3. Materials and Methods

3.1. Chemicals

Sulfamethazine ($C_{11}H_{14}O_2N_4S$, 4-Amino-*N*-(4,6-dimethyl-2-pyrimidinyl) benzenesulfonamide) was a product of Sigma-Aldrich Chemie GmbH (Taufkirchen, Germany) and was used as received.

TiO_2 was from Degussa-Hüls AG (Frankfurt, Germany) (TiO_2 P-25 Degussa, anatase/rutile: 3.6/1, BET surface area 56 m^2 g^{-1}, nonporous). H_2SO_4 and NaOH used for pH adjustment, as well as anhydrous Na_2SO_4 (p. a. > 99%), were from Merck (Darmstadt, Germany). Ti plates (0.5 mm thick) were from Alfa Aesar (Tewksbury, MA, USA) (99.5% metal basis). Doubly distilled water was used for this study. Aqueous stock solutions of sulfamethazine (200 mg L^{-1}) were prepared weekly, protected from light, and stored at 25 °C.

3.2. TiO_2/Ti Electrode Preparation

The procedure for the preparation of TiO_2/Ti electrodes has been previously described in detail [34,47]. Various parameters, e.g., the preparation method, heat treatment conditions, etc., affect the photoelectrochemical efficiency of a TiO_2 electrode. In our study, by using the dip coating method, the best results regarding the photoelectrocatalytic efficiency were recorded for specimens treated between 400 and 700 °C and for time intervals of 1.5 to 10 h with electrodes annealed at 500 °C for 1.5 h. Thus, all bulk photoelectrocatalytic experiments on SMT degradation were performed using these electrodes.

3.3. Experimental Setup and Procedures

For the electrochemical/photoelectrochemical characterization of the produced TiO_2 films, a classical three-compartment photoelectrochemical cell was used.

The detailed experimental setup and the electrochemical reactor for the bulk photoelectrolysis experiments have been described previously [48]. It consisted of a 500 cm^3 cylindrical cell (i.d. = 7.8 cm; height = 14.8 cm) with a removable cap. The same Osram Dulux 9 W/78 UVA lamp was placed in a cylindrical borosilicate glass sleeve and introduced in the middle of the reactor. The light intensity on the TiO_2 electrode surface position was measured as 3.9 mW cm^{-2} with a photometer (Solar Light Co., Glenside, PA, USA, PMA 2100), while the flux of the UV-A photons emitted into the 340 cm^3 reaction solution was found to be 1.25×10^{-4} Einstein L^{-1} min^{-1} by ferrioxalate actinometry [30]. The TiO_2/Ti electrode with a 220 cm^2 surface area was fitted between the cylindrical sleeve and the inner wall of the cell. A stainless steel wire was coiled around the sleeve and used as a counter electrode, while an Ag/AgCl electrode equipped with a salt bridge made of

a thin thermoplastic tube ending in a Vycor® tip was used as a reference electrode. The potentiostat Wenking POS 73 (Bank Elektronik, Pohlheim, Germany) was used to obtain the applied potential. The photoelectrochemical reactor was placed in a dark chamber in order to avoid interference from the daylight. All experiments were carried out at a temperature of 25 °C.

To check the reproducibility of the experimental results, some photocatalytic experiments were repeated three times. The reproducibility of the optical density values was within ±5%, while that of the dissolved organic carbon (DOC) ± 10%.

3.4. Analytical Methods

Scanning Electron Microscopy (SEM) was carried out using a JSM 733 microscope (Tokyo, Japan). A SHIMADZU X-ray diffractometer (Lab X, XRD-6000, Kyoto, Japan) was used for X-ray diffraction (XRD) coating characterization.

Absorption spectra in the ultraviolet and visible ranges were recorded with a Shimadzu PharmaSpec UV-100 spectrophotometer (Kyoto, Japan). A total organic carbon analyzer (Shimadzu Instruments, model V_{CSH} TOC Analyzer, Kyoto, Japan) was used to monitor the dissolved organic carbon (DOC) reduction. During the degradation experiments, samples of 5 mL for the absorption spectra and 6 mL for the DOC analysis were collected from the reactor at the determined time intervals.

4. Conclusions

In this work, the photoelectrocatalytic oxidative degradation of sulfamethazine, a sulfonamide drug, has been studied under artificial illumination in a novel photoelectrocatalytic reactor. It has been proven that the particulate TiO_2/Ti electrode could be efficient for degradation and mineralization, despite the fact that more active electrodes are required for practical achievement. The degradation efficiency is faster by photoelectrocatalysis compared to photocatalysis or electrochemical oxidation alone. This finding supports the fact that there is a synergetic effect on SMT degradation when an appropriate irradiation and a potential difference are applied simultaneously on the particulate TiO_2/Ti electrode, leading to a 153% increase in the rate constant of degradation and a 298% increase in the rate constant of mineralization in comparison to the simple photocatalytic process. The SMT photooxidation followed first-order kinetics according to the Langmuir–Hinshelwood model, while parameters such as pH, concentration of the target drug molecule, and applied potential play a key role in influencing the reaction rate constant.

Author Contributions: Conceptualization, I.P.; data curation, N.P., E.P., S.S., P.K., D.M. and I.P.; formal analysis, N.P. and E.P.; funding acquisition, I.P.; investigation, N.P., E.P. and S.S.; methodology, S.S. and I.P.; project administration, I.P.; software, N.P., E.P. and P.K.; supervision, S.S., D.M. and I.P.; validation, N.P., E.P. and S.S.; visualization, N.P. and E.P.; writing—review and editing, N.P., P.K., D.M., S.S. and I.P. All authors have read and agreed to the published version of the manuscript.

Funding: This research received no external funding.

Data Availability Statement: Not applicable.

Conflicts of Interest: The authors declare no conflict of interest.

References

1. Council of the European Union. Council Directive 2000/60/EC of October 2000 establishing a framework for Community action in the field of water policy. *Off. J. Eur. Union* **2000**, *L327*, 1–72.
2. Herrmann, J.-M. Photocatalysis fundamentals revisited to avoid several misconceptions. *Appl. Catal. B* **2010**, *99*, 461–468. [CrossRef]
3. Friedmann, D.; Mendiveb, C.; Bahnemann, D. TiO_2 for water treatment: Parameters affecting the kinetics and mechanisms of photocatalysis. *Appl. Catal. B* **2010**, *99*, 398–406. [CrossRef]
4. Kaneko, M.; Okura, I.E. (Eds.) *Photocatalysis: Science and Technology*; Springer: New York, NY, USA, 2002; ISBN 3-540-43473-9.
5. Xin, Y.; Liu, H.; Han, L.; Zhou, Y. Comparative study of photocatalytic and photoelectrocatalytic properties of alachlor using different morphology TiO_2/Ti photoelectrodes. *J. Hazard. Mater.* **2011**, *192*, 1812–1818. [CrossRef]

6. Brugnera, M.F.; Rajeshwar, K.; Cardoso, J.C.; Zanoni, M.V.B. Bisphenol A removal from wastewater using self-organized TiO_2 nanotubular array electrodes. *Chemosphere* **2010**, *78*, 569–575. [CrossRef] [PubMed]
7. Xu, Y.; Jia, J.; Zhong, D.; Wang, Y. Degradation of dye wastewater in a thin-film photoelectrocatalytic (PEC) reactor with slant-placed TiO_2/Ti anode. *Chem. Eng. J.* **2009**, *150*, 302–307. [CrossRef]
8. Krýsa, J.; Zlamal, M.; Waldner, G. Effect of oxidisable substrates on the photoelectrocatalytic properties of thermally grown and particulate TiO_2 layers. *J. Appl. Electrochem.* **2007**, *37*, 1313–1319. [CrossRef]
9. Tzeng, T.W.; Wang, S.L.; Chen, C.C.; Tan, C.C.; Liu, Y.T.; Chen, T.Y.; Tzou, Y.M.; Chen, C.C.; Hung, J.T. Photolysis and photocatalytic decomposition of sulfamethazine antibiotics in an aqueous solution with TiO_2. *RSC Adv.* **2016**, *6*, 69301–69310. [CrossRef]
10. Aissani, T.; Yahiaoui, I.; Boudrahem, F.; Ait Chikh, S.; Aissani-Benissad, F.; Amrane, A. The combination of photocatalysis process (UV/TiO_2(P25) and UV/ZnO) with activated sludge culture for the degradation of sulfamethazine. *Sep. Sci. Technol.* **2018**, *53*, 1423–1433. [CrossRef]
11. Fukahori, S.; Fujiwara, T. Modeling of sulfonamide antibiotic removal by TiO_2/high-silica zeolite HSZ-385 composite. *J. Hazard. Mater.* **2014**, *272*, 1–9. [CrossRef]
12. Vanlalhmingmawia, C.; Tiwari, D.; Kim, D.J. Novel nanocomposite thin film in the efficient removal of antibiotics using visible light: Insights of photocatalytic reactions and stability of thin film in real water implications. *Environ. Res.* **2023**, *218*, 115007. [CrossRef]
13. Zhang, Y.; He, Z.; Zhou, J.; Huang, Y.; Li, W.; Li, Y.; Li, Y.; Bi, H.; Chang, F.; Zhang, H.; et al. Amorphous Co@TiO_2 heterojunctions: A high-performance and stable catalyst for the efficient degradation of sulfamethazine via peroxymonosulfate activation. *Chemosphere* **2022**, *307*, 135681. [CrossRef]
14. Fukahori, S.; Fujiwara, T. Photocatalytic decomposition behavior and reaction pathway of sulfamethazine antibiotic using TiO_2. *J. Environ. Manag.* **2015**, *157*, 103–110. [CrossRef]
15. Babić, S.; Zrnčić, M.; Ljubas, D.; Ćurković, L.; Škorić, I. Photolytic and thin TiO_2 film assisted photocatalytic degradation of sulfamethazine in aqueous solution. *Environ. Sci. Pollut. Res.* **2015**, *22*, 11372–11386. [CrossRef] [PubMed]
16. Jia, M.; Yang, Z.; Xu, H.; Song, P.; Xiong, W.; Cao, J.; Zhang, Y.; Xiang, Y.; Hu, J.; Zhou, C.; et al. Integrating N and F co-doped TiO_2 nanotubes with ZIF-8 as photoelectrode for enhanced photo-electrocatalytic degradation of sulfamethazine. *Chem. Eng. J.* **2020**, *388*, 124388. [CrossRef]
17. Zhang, J. Degradation mechanism of Sulfa drugs based on theoretical prediction and experimental examination in TiO_2 suspension. *Res. Chem. Intermed.* **2014**, *40*, 1089–1102. [CrossRef]
18. Hu, Z.; Liang, R.; Song, X.; Wu, H.; Sun, J.; Liu, J.; Zhou, M.; Arotiba, O.A. Efficient Bias-Free Degradation of Sulfamethazine by TiO_2 Nanoneedle Arrays Photoanode and Co_3O_4 Photocathode System under LED-Light Irradiation. *Catalysts* **2023**, *13*, 327. [CrossRef]
19. Zhou, Q.; Fang, Z. Highly sensitive determination of sulfonamides in environmental water samples by sodium dodecylbenzene sulfonate enhanced micro-solid phase extraction combined with high performance liquid chromatography. *Talanta* **2015**, *141*, 170–174. [CrossRef]
20. Zeng, X.; Shu, S.; Meng, Y.; Wang, H.; Wang, Y. Enhanced photocatalytic degradation of sulfamethazine by g-C_3N_4/Cu, N-TiO_2 composites under simulated sunlight irradiation. *Chem. Eng. J.* **2023**, *456*, 141105. [CrossRef]
21. Qi, L.; Zhang, H.; Xiao, C.; Ni, L.; Chen, S.; Qi, J.; Zhou, Y.; Zhu, Z.; Li, J. Improvement of peroxymonosulfate utilization efficiency for sulfamethazine degradation by photo-electron activating peroxymonosulfate: Performance and mechanism. *J. Colloid Interface Sci.* **2023**, *633*, 411–423. [CrossRef]
22. Wang, N.; Li, X.; Yang, Y.; Guo, T.; Zhuang, X.; Ji, S.; Zhang, T.; Shang, Y.; Zhou, Z. Enhanced photocatalytic degradation of sulfamethazine by Bi-doped TiO_2 nano-composites supported by powdered activated carbon under visible light irradiation. *Sep. Purif. Technol.* **2019**, *211*, 673–683. [CrossRef]
23. Fouad, K.; Gar Alalm, M.; Bassyouni, M.; Saleh, M.Y. A novel photocatalytic reactor for the extended reuse of W–TiO_2 in the degradation of sulfamethazine. *Chemosphere* **2020**, *257*, 127270. [CrossRef] [PubMed]
24. Mendiola-Alvarez, S.Y.; Hernández-Ramírez, A.; Guzmán-Mar, J.L.; Maya-Treviño, M.L.; Caballero-Quintero, A.; Hinojosa-Reyes, L. A novel P-doped Fe_2O_3 -TiO_2 mixed oxide: Synthesis, characterization and photocatalytic activity under visible radiation. *Catal. Today* **2019**, *328*, 91–98. [CrossRef]
25. Payan, A.; Akbar Isari, A.; Gholizade, N. Catalytic decomposition of sulfamethazine antibiotic and pharmaceutical wastewater using Cu-TiO_2@functionalized SWCNT ternary porous nanocomposite: Influential factors, mechanism, and pathway studies. *Chem. Eng. J.* **2019**, *361*, 1121–1141. [CrossRef]
26. Ji, H.; Du, P.; Zhao, D.; Li, S.; Sun, F.; Duin, E.C.; Liu, W. 2D/1D graphitic carbon nitride/titanate nanotubes heterostructure for efficient photocatalysis of sulfamethazine under solar light: Catalytic "hot spots" at the rutile–anatase–titanate interfaces. *Appl. Catal. B* **2020**, *263*, 118357. [CrossRef]
27. Vilar, V.J.P.; Pillai, S.C.; Poulios, I.; Mantzavinos, D.; Pintar, A. Advanced oxidation processes: Recent achievements and perspectives. *Environ. Sci. Pollut. Res.* **2020**, *27*, 22141–22143. [CrossRef]
28. Wu, H.; Hu, Z.; Liang, R.; Nkwachukwu, O.V.; Arotiba, O.A.; Zhou, M. Novel $Bi_2Sn_2O_7$ quantum dots/TiO_2 nanotube arrays S-scheme heterojunction for enhanced photoelectrocatalytic degradation of sulfamethazine. *Appl. Catal. B* **2023**, *321*, 122053. [CrossRef]

29. Candia-Onfray, C.; Irikura, K.; Calzadilla, W.; Rojas, S.; Boldrin Zanoni, M.V.; Salazar, R. Degradation of contaminants of emerging concern in a secondary effluent using synthesized MOF-derived photoanodes: A comparative study between photo-, electro- and photoelectrocatalysis. *Chemosphere* **2023**, *315*, 137683. [CrossRef]
30. Braun, A.M.; Maurette, M.; Oliveros, E. *Photochemical Technology*; Wiley: New York, NY, USA, 1991.
31. Licht, S. Semiconductor Electrodes and Photoelectrochemistry. In *Encyclopedia of Electrochemistry*; Bard, A., Stratmann, M., Eds.; Wiley-VCH: Weinheim, Germany, 2002; Volume 6.
32. Memming, R. *Semiconductor Electrochemistry*; Wiley-VCH: Weinheim, Germany, 2001.
33. Pleskov, Y.; Gurevich, Y. *Semiconductor Photoelectrochemistry*; Springer: New York, NY, USA, 1986.
34. Mintsouli, I.; Philippidis, N.; Poulios, I.; Sotiropoulos, S. Photoelectrochemical characterisation of thermal and particulate titanium dioxide electrodes. *J. Appl. Electrochem.* **2006**, *36*, 463–474. [CrossRef]
35. Alulema-Pullupaxi, P.; Espinoza-Montero, P.J.; Sigcha-Pallo, C.; Vargas, R.; Fernández, L.; Peralta-Hernández, J.M.; Paz, J.L. Fundamentals and applications of photoelectrocatalysis as an efficient process to remove pollutants from water: A review. *Chemosphere* **2021**, *281*, 130821. [CrossRef]
36. Daghrir, R.; Drogui, P.; Robert, D. Photoelectrocatalytic technologies for environmental applications. *J. Photochem. Photobiool. A* **2012**, *238*, 41–52. [CrossRef]
37. Cunningham, J.; Al-Sayyed, G.; Srijaranai, S. Adsorption of model pollutants onto TiO_2 particles in relation to photoremedation of contaminated water. In *Aquatic and Surface Photochemistry*; Helz, G., Zepp, R., Crosby, D., Eds.; Chapter 2; CRC Press: Boca Raton, FL, USA, 1994; pp. 317–348.
38. Turchi, C.S.; Ollis, D.F. Photocatalytic degradation of organic-water contaminants—mechanisms involving hydroxyl radical attack. *J. Catal.* **1990**, *122*, 178–192. [CrossRef]
39. Akpan, U.G.; Hameed, B.H. Parameters affecting the photocatalytic degradation of dyes using TiO_2-based photocatalysts: A review. *J. Hazard. Mater.* **2009**, *170*, 520–529. [CrossRef]
40. Kesselman, J.; Lewis, N.; Hoffmann, M. Photoelectrochemical degradation of 4-chlorocatechol at TiO_2 electrodes: Comparison between sorption and reactivity. *Environ. Sci. Technol.* **1997**, *31*, 2298. [CrossRef]
41. Yang, S.; Liu, Y.; Sun, C. Preparation of anatase TiO_2/Ti nanotube-like electrodes and their high photoelectrocatalytic activity for the degradation of PCP in aqueous solution. *Appl. Catal. A Gen.* **2006**, *301*, 284–291. [CrossRef]
42. Kim, D.H.; Anderson, M.A. Solution factors affecting the photocatalytic and photoelectrocatalytic degradation of formic acid using supported TiO_2 thin films. *J. Photochem. Photobiol. A* **1996**, *94*, 221–229. [CrossRef]
43. Liu, X.; Ji, H.; Li, S.; Liu, W. Graphene modified anatase/titanate nanosheets with enhanced photocatalytic activity for efficient degradation of sulfamethazine under simulated solar light. *Chemosphere* **2019**, *233*, 198–206. [CrossRef] [PubMed]
44. Ayala-Durán, S.C.; Hammer, P.; Pupo Nogueira, R.F. Surface composition and catalytic activity of an iron mining residue for simultaneous degradation of sulfonamide antibiotics. *Environ. Sci. Pollut. Res.* **2020**, *27*, 1710–1720. [CrossRef]
45. Kraeutler, B.; Bard, A.J. Heterogeneous photocatalytic preparation of supported catalysts—Photodeposition of platinum on TiO_2 powder and other substrates. *J. Am. Chem. Soc.* **1978**, *100*, 4317–4318. [CrossRef]
46. Zhao, W.; Duan, J.; Ji, B.; Ma, L.; Yang, Z. Novel formation of large area N-TiO_2/graphene layered materials and enhanced photocatalytic degradation of antibiotics. *J. Environ. Chem. Eng.* **2020**, *8*, 102206. [CrossRef]
47. Philippidis, N.; Nikolakaki, E.; Sotiropoulos, S.; Poulios, I. Photoelectrocatalytic inactivation of *E. coli* XL-1 blue colonies in water. *J. Chem. Technol. Biotechnol.* **2010**, *85*, 1054–1060. [CrossRef]
48. Philippidis, N.; Sotiropoulos, S.; Efstathiou, A.; Poulios, I. Photoelectrocatalytic degradation of the insecticide imidacloprid using TiO_2/Ti electrodes. *J. Photochem. Photobiol.* **2009**, *204*, 129–136. [CrossRef]

Disclaimer/Publisher's Note: The statements, opinions and data contained in all publications are solely those of the individual author(s) and contributor(s) and not of MDPI and/or the editor(s). MDPI and/or the editor(s) disclaim responsibility for any injury to people or property resulting from any ideas, methods, instructions or products referred to in the content.